

EFFECTS OF SUPPORT STRUCTURE DYNAMICS ON CENTRIFUGAL COMPRESSOR ROTOR RESPONSE

Stefano Rossin

Consulting Engineer
GE Oil&Gas
Via Felice Matteucci 2
Florence, Italy
stefano.rossin@ge.com

Francesco Capanni

Senior Engineer
GE Oil&Gas
Via Felice Matteucci 2
Florence, Italy
francesco.capanni@ge.com

Daniele Panara

Lead Engineer
GE Oil&Gas
Via Felice Matteucci 2
Florence, Italy
daniele.panara@ge.com

Andrea Rindi

Professor
Industrial Engineering University
Via Di Santa Marta 3
Florence, Italy
andrea.rindi@unifi.it

Enrico Meli

Assistant Professor
Industrial Engineering University
Via Di Santa Marta 3
Florence, Italy
enrico.meli@unifi.it

Giovanni Pallini

PhD Student
Industrial Engineering University
Via Di Santa Marta 3
Florence, Italy
giovanni.pallini@unifi.it



Stefano Rossin is consulting engineer for centrifugal compressors, gas turbines and industrial plants mechanical structures in GE Oil&Gas. He holds a master degree in aeronautical engineering and has 16 years of experience in structural dynamics. He is author of more than 10 international papers and 2 patents in the Oil&Gas field.

ABSTRACT

Accurate modeling of complicated dynamic phenomena characterizing rotating machineries represents a critical aspect in the rotor dynamic field. A correct prediction of rotor behavior is fundamental to identify safe operating conditions avoiding unstable operating range that may lead to erroneous project solution or possible unwanted consequences for the plant.

Considering generic rotating machineries as mainly partitioned in four components (rotors, bearings, stator and supporting structure), most research activities have been addressed so far with strong focus more on the single components rather than on the whole system assembly.

The importance of a combined analysis of rotors and elastic supporting structure (Kruger 2013) arises with the continuous development of turbo machinery applications, in particular in the Oil & Gas field, where a wide variety of solutions, such as off-shore installations or modularized turbo compression and turbo generator trains, lead to the need of a more complete study not only limited to the rotor-bearing system.

Complex elastic systems (see general architecture at Figure 1) in some situations might strongly dominate the entire shaft line rotor dynamic response (mode shapes, resonance frequencies and unbalance response). They give birth to transfer functions which introduce strong coupling phenomena (Cavalca 2015) between machines bearings, becoming enablers of a new shaft line dynamics.

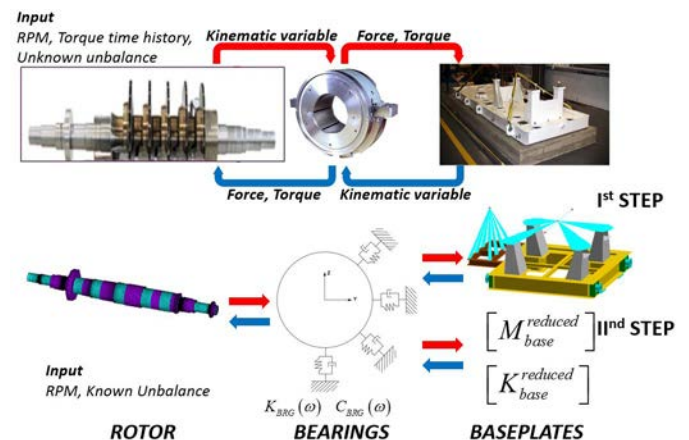


Figure 1: general architecture

Such situation was detected in a centrifugal compressor installed on-shore on concrete foundations, where the machine was unable to reach the nominal speed due to excessive shaft vibration detected at the proximity probes.

After several attempts to realign the entire compression train shaft line and multiple checks on the rotor residual unbalance, the successful steps of the investigation highlighted the

likelihood of rotor to structure interaction potentially driven by a weak structure anchoring system.

Unlike established procedures based on existing methodologies often requiring expensive computational time and/or unwanted level of detail, this work attempts to rise the requirement of a new method leveraging a high level of accuracy / high computationally efficient method emphasizing a valuable match between experimental and numerical results which confirms the importance of a proper definition of the complex transfer function.

INTRODUCTION

A general rotordynamic assembly is composed of three components:

- Rotor
- Bearings
- Support structure.

As the request for high efficiency with great expectation on systems size and weight is nowadays increasing, compression and power train structures must necessarily become much lighter and consequently more flexible. The introduction of components in the assembly that cannot be considered absolutely rigid, led to the need of a deeper study of the dynamic behaviour of rotating machines to guarantee a safe operating range. When looking at the supporting structure anchoring system for off shore installation, the iso-static solutions, highlighted in Figure 2, is characterizing the way long common support structures are often bounded to the ground. This is obtained through the usage of hinge and spherical joints, which allow barge deck deflection and baseplate thermal growth, but unfortunately at the same time introduce unwanted complex response of the rotating equipment (turbo compressor, turbo-generator, moto-compressor...).

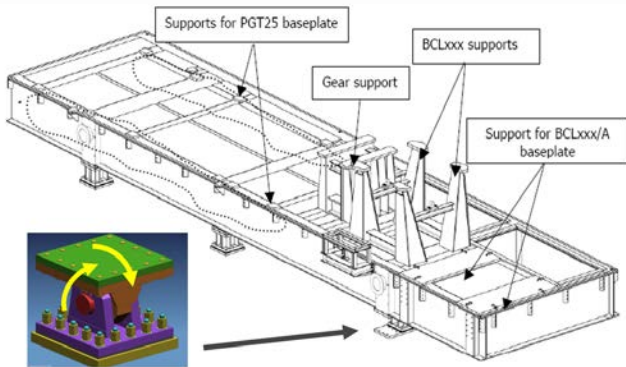


Figure 2: support structure and anchoring system

Practical engineering rules are often introduced based on international standards such as ISO or API, to estimate whether structurally wise the rotating equipment is properly supported. When looking at the Figure 3 for instance, one can compare the stiffness of the supporting structure at a specific location, usually one of the bearings seat, with a limit defined upon the maximum expected vibration under the maximum unbalance load. According to such criteria any potential lack of stiffness

can be highlighted, such as in Figure 3 for the baseplate under investigation: the lack of stiffness at 20 and 30 Hz (1200 and 1800rpm) corresponds to a possible resonance of the compressor assembly due to the compressor supporting structure elasticity.

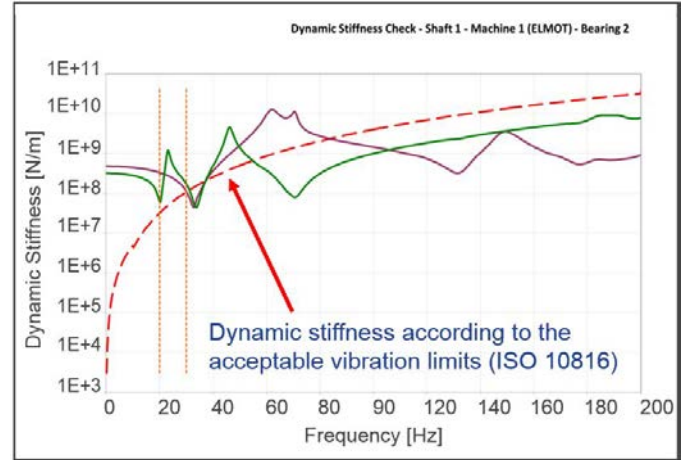


Figure 3: dynamic stiffness acceptance threshold

In accordance with the baseplate stiffness function, it is also important to underline that the complexity of the supporting structure response (Kang 2000), that comes out when the deformed shapes of the supporting structure enhance the linking between bearings on the same shaft line (Figure 4), should give enough information to reproduce the linking between different DOFs and the linking between the DOF of different bearings on the shaft line.

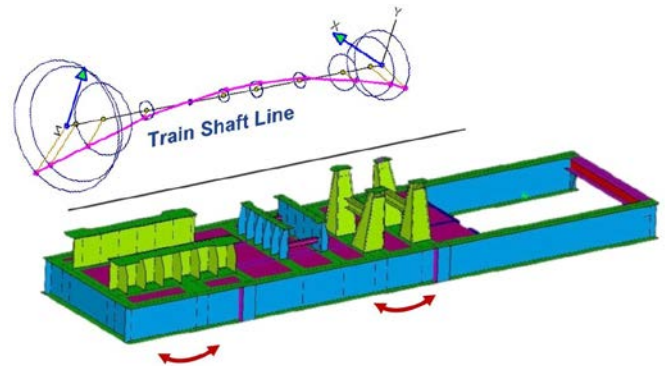


Figure 4: rotor train mode shape involving crosstalk terms

How to introduce the complex behaviour of the support system considering an equivalent dynamical model? It is necessary to decompose the transfer function (Cuppens 2000) of an equivalent baseplate in two main components (Figure 5): direct and cross-talking terms.

For a simple single rotor it is possible to define a general transfer function matrix (T_f) as composed of four sub elements. As visible in Figure 5, direct terms ($T_{f_{11}}$ and $T_{f_{22}}$) represent those T_f s in series with the bearings characteristic, while cross-talking terms ($T_{f_{12}}$ and $T_{f_{21}}$) represent those functions coupling the dynamic behaviour of the two bearings. Cross-talking terms can be considered peculiar of second rocking and flexible deformed shape, characteristic of elastic support structure like off-shore installation, where the response of bearings on the

same shaft line cannot be considered separated.

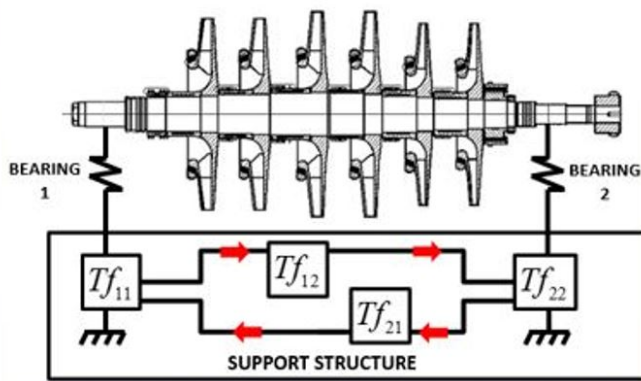


Figure 5: transfer function representation

Two steps are required to accomplish the analysis and to study the effect of the support structure on the rotor dynamic:

- Build a complete model without simplification to have a reference point;
- Build an equivalent accurate and efficient model to separate the influence of different component and different degree of freedom.

The complete model considers the rotor mounted on foundations and nothing is subject to any sort of model simplification. The reduced model leads instead to the reduction of calculation time introducing simplifying assumption (equivalent transfer function) to represent the supporting structure, trying to obtain the maximum accuracy with a higher level of efficiency than the original model. The importance of this study relies on the necessity to obtain an accurate and efficient tool able to supply a good compromise between poor and too complex modelling of the whole rotordynamic assembly.

A graphic representation of the general architecture is visible in Figure 1. The first line in Figure 1 represents the physical/real system and the second line stands for the equivalent FEM model. The general architecture diagram shows the flux of variables between the three main components of the assembly: it is possible to recognize that bearings represents the means to transmit a continuous flow of action and reaction forces between rotor and baseplate. In particular, the unbalance force, that moves the rotor in a set of different positions, causes an excitation of the elastic supporting structure that in turn react according to its resonance frequencies, while bearings represent the means of communication.

As the rotor and all the system correspond to a full 3D system, the displacement will be explicitly present in their 3 directions x , y and z , respectively on the longitudinal axis parallel to the symmetry axis of the rotor, transversal and in the vertical direction. The three translations take with them the three rotations ϑ_x , ϑ_y and ϑ_z .

The first step of the analysis considers that all elements are fully described considering nodal degrees of freedom and no simplification have been applied to reduce the dimension of the mathematical problem to solve.

The FEM assembly is modelled using the Ansys suit, especially the Ansys Parametric Design Language (APDL).

The Complete model is a full three-dimensional assembly of

rotor, supporting structure and bearings.

The main component of the assembly is the rotor shaft. It is modelled with a Timoshenko based beam with circular cross section and has 6 DOFs per node. The shaft is described separating the stiffness and mass contributions of its various portions by specifying two different materials: a first material with full steel properties and a second material to just add mass ad obtain the real description of the element. The rotor is the sum of many contributes and it must keep into account the effect of the keyed and shrink fitted elements, this contribute is implemented as concentrated mass and inertia suitably distributed along the length of the shaft.

Bearings are another fundamental and critical component to be modelled, they are described by a damping and a stiffness matrix dependent on the rotating frequency of the rotor. Reactions forces due to bearings interaction undergo the hypothesis of nodal concentration so that the bearing is considered an element with no axial length: that assumption can be considered valid if the area of bearings interaction is compared to the whole shaft surface. The mass and the inertia of the bearing is considered negligible.

Following a description of the model that starts around the rotor, the next element is the rotor casing. This element is considered infinitely rigid respect to all the other components and so it is dynamically approximated with concentrated properties of mass and inertia applied to his own centre of gravity. To represent the rotor enclosure as a rigid element is a legitimate hypothesis when the thickness of shells that contain the rotor overpass a certain margin, furthermore casing in heavy duty application are usually casting product of few components and high stiffness is clearly more than an hypothesis in relation to the nearby elements.

The entire baseplate is constructed with shell elements and the stiffness of the anchoring spring to the ground is extracted from dynamic stiffness simulations to satisfy the results of hammer test on the supporting pedestals.

THE MODEL

In this paragraph, equations and hypothesis are explicitly expressed to better understand the FEM model that stand behind results.

Even though the implemented model is used for a stationary analysis a transitory simulation is already possible and planned in anticipation of future comparison and studies.

The Rotor

The complete rotor is its self a component parted in subassembly, as it would be in the real plant if we suppose to key and shrink over the naked shaft: impellers that transform the energy derived from the fluid, element of junction to transmit wrench and get the machine running and other sleeves elements.

Every supplementary element linked to the shaft is characterized with E (Young modulus), ρ (density), m_x , m_y , m_z , I_p , I_t and consequently with the required matrix M , K and G respectively mass, stiffness and gyroscopic effect matrices. Finally, it is now possible to write the complete equation that comes from Jeffcott's theory in a summarized array:

$$M_r \ddot{q}_r + (Cr + \Omega G_r) \dot{q}_r + K_r q_r = F_r^{brg} + F_r^{ext} \quad (1)$$

With the subscript r it is possible to recognize all the matrix, vectors and coefficients related to the rotor, this notation will be useful when the system will include the dynamic contribute of the supporting structure. In Eq.(1) F_r^{brg} represents the contribute of the bearings reaction forces and F_r^{ext} is the vector that gather all external loads.

Looking in detail to the expression that represent the dynamic of the rotor it is helpful to part all degree of freedom in two categories

$$q_r = \{q_{rb}^T, q_{rg}^T\}^T \quad q_s = \{q_{sb}^T, q_{sg}^T\}^T \quad (2)$$

where r refers to the rotor, s to the support structure and the letter b and g respectively represent the DOFs related to the nodes belonging to the bearing interface and all the residual DOFs (general node DOF).

To validate the beam model a sensitivity mesh analysis has been performed to choose the right node spacing (the minimum dimension of the element) in accordance with accuracy of results and efficiency.

Bearings

Bearings represent a complex component to model and a multiphysics object to study (Brugier 1989), which must keep into account thermal and structural characteristics and behaviour.

A common linearised representation of bearings following literature example is reported in Figure 6. The forces that the bearings exert on the rotor can be expressed in terms of linearised force coefficients for small perturbations about a stationary equilibrium at a given shaft speed.

The forces are expanded as follows when the transversal plane is described by the direction of the Z and Y :

$$F_{brg}(\omega) = \begin{Bmatrix} F_x(\omega) \\ F_y(\omega) \\ F_z(\omega) \end{Bmatrix} = \begin{bmatrix} -K_{xx}(\omega) & 0 & 0 \\ 0 & -K_{yy}(\omega) & -K_{yz}(\omega) \\ 0 & -K_{zy}(\omega) & -K_{zz}(\omega) \end{bmatrix} \begin{Bmatrix} q_{xrb} - q_{xsb} \\ q_{yrb} - q_{ysb} \\ q_{zrb} - q_{zsb} \end{Bmatrix} + \begin{bmatrix} -C_{xx}(\omega) & 0 & 0 \\ 0 & -C_{yy}(\omega) & -C_{yz}(\omega) \\ 0 & -C_{zy}(\omega) & -C_{zz}(\omega) \end{bmatrix} \begin{Bmatrix} \dot{q}_{xrb} - \dot{q}_{xsb} \\ \dot{q}_{yrb} - \dot{q}_{ysb} \\ \dot{q}_{zrb} - \dot{q}_{zsb} \end{Bmatrix} \quad (3)$$

Direct stiffness coefficients, K_{yy} , K_{zz} produce a radial force directed inward and co-linear with the rotor deflection vector. If the coefficients are negative, the direction of the force reverses (outward). The *direct damping coefficients*, C_{yy} and C_{zz} produce a tangential force normal to the rotor deflection vector and opposing the whirl velocity when their sign is positive and otherwise when their sign turns negative.

Cross-coupled stiffness coefficients K_{yz} , K_{zy} are responsible of a tangential force normal to the deflection vector and with direction dependent on the algebraic signs.

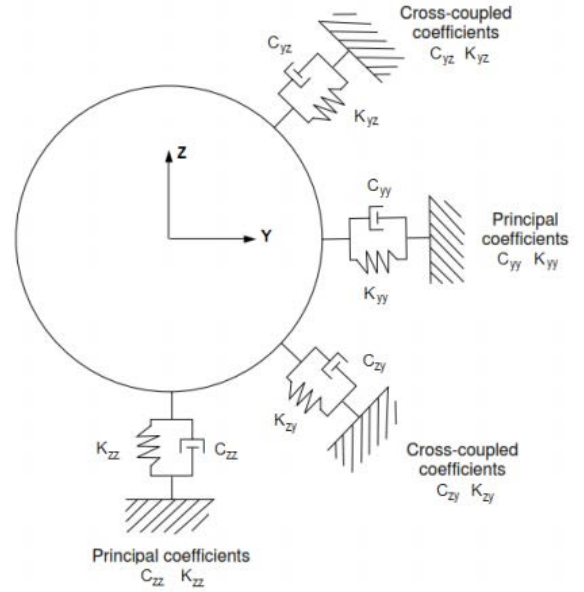


Figure 6: bearing representation

The combination $K_{yz} > 0$, $K_{zy} < 0$ yield to forward whirl and can be destabilizing. Cross-coupled stiffness coefficients with the same sign are slightly stabilizing, as they make the orbit elliptical.

Cross-coupled damping coefficients C_{yz} , C_{zy} are responsible of radial force co-linear with the deflection vector and with direction dependent on the algebraic signs, either stiffening or softening.

It is known that instability may occur due to the presence of skew-symmetric stiffness coefficients (cross coupling terms). In a tilting-pad journal bearing, by eliminating cross-coupled stiffness coefficients it is possible to prevent this instability problem. In order to improve the stability of a circular bearing, a potential solution is to change the geometrical configuration by using, for example, a pressure-dam bearing, elliptical bearing, and multi-lobe bearing.

In Eq.(3) it is possible to recognize that in K and C matrix the constraint in the axial direction is uncoupled from the transversal boundary condition, this choice derive from the partition of axial and lateral load on different bearing, a couple able to bear axial thrust and a couple able to react to vertical and lateral displacements.

To evaluate the real response of the assembly K and C matrix are frequency dependent (ω is the rotational velocity of the shaft) to compensate axial load and centrifugal effects.

Elastic support structure

The baseplate is a sum of different elements: *shell* to model the steel structure, *rigid connections* to represent joints between rotor and baseplate and to describe the casing.

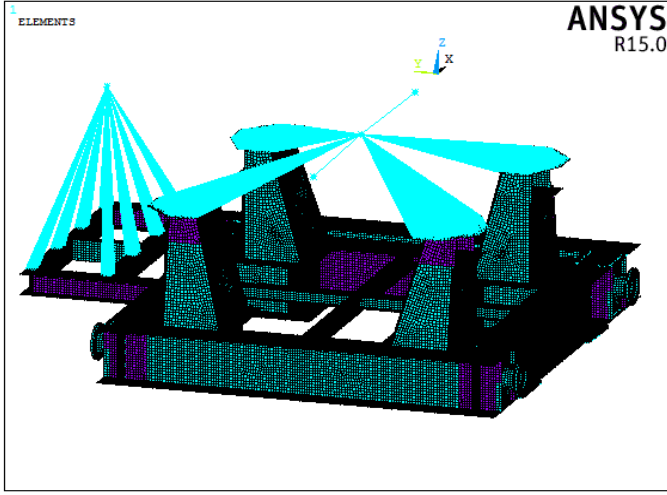


Figure 7: test case support structure

To use Shell elements to model steel structure composed of welded plate is a common practice: it means to extract the mid surface of the real steel plate and then associate the thickness to have an approximation of the result on the third dimension (the thickness indeed). It is clear that this approximation combine accuracy and efficiency when thickness becomes negligible respect to other dimensions, therefore when bodies are nearer to a 2D representation and a 3D model would result too expensive in time of calculation and may lead to bad conditioned solid modelling.

This first step of the analysis represents the main comparison term between the accelerometer data and the simulated result. This first step represents the validation of the FEM model.

To verify that the analysis run in an allowed range a mesh sensitivity study has been performed on the dimension of the shell elements and on the distribution of nodes in accordance of mesh quality parameter.

It is now to write once again the equation that describe the motion of the baseplate assembly

$$M_s \ddot{q}_s + C_s \dot{q}_s + K_s q_s = F_s^{ext} + F_s^{brg}. \quad (4)$$

In Eq.(4) F_s^{ext} represents a general external load, F_s^{brg} consider the reaction forces exchanged with bearings, M_s , C_s , K_s the mass, stiffness and damping matrix of the baseplate.

Complete model

To describe the dynamic of the whole system, it is helpful to introduce a new set of coordinate \bar{q} , which corresponds to a rearrangement of the vector containing the coordinate of the node related to the rotor and to the support structure.

In Eq.(5) F^{ext} this time contains all the external forces, that in the specific case will represent unbalance load configuration. At this point, it is helpful to write the complete equation of the assembly:

$$\begin{aligned} & \begin{bmatrix} M_r^{bb} & M_r^{bg} & 0 & 0 \\ M_r^{gb} & M_r^{gg} & 0 & 0 \\ 0 & 0 & M_s^{bb} & M_s^{bg} \\ 0 & 0 & M_s^{gb} & M_s^{gg} \end{bmatrix} \begin{Bmatrix} \ddot{q}_{rb} \\ \ddot{q}_{rg} \\ \ddot{q}_{sb} \\ \ddot{q}_{sg} \end{Bmatrix} + \\ & + \begin{bmatrix} C_r^{bb} + C^{brg} & C_r^{bg} & -C^{brg} & 0 \\ C_r^{gb} & C_r^{gg} & 0 & 0 \\ -C^{brg} & 0 & C_s^{bb} + C^{brg} & C_s^{bg} \\ 0 & 0 & C_s^{gb} & C_s^{gg} \end{bmatrix} + \Omega \begin{bmatrix} G_r^{bb} & 0 & 0 & 0 \\ 0 & G_r^{gg} & 0 & 0 \\ 0 & 0 & 0 & 0 \\ 0 & 0 & 0 & 0 \end{bmatrix} \begin{Bmatrix} \dot{q}_{rb} \\ \dot{q}_{rg} \\ \dot{q}_{sb} \\ \dot{q}_{sg} \end{Bmatrix} + \\ & + \begin{bmatrix} K_r^{bb} + K^{brg} & K_r^{bg} & -K^{brg} & 0 \\ K_r^{gb} & K_r^{gg} & 0 & 0 \\ -K^{brg} & 0 & K_s^{bb} + K^{brg} & K_s^{bg} \\ 0 & 0 & K_s^{gb} & K_s^{gg} \end{bmatrix} \begin{Bmatrix} q_{rb} \\ q_{rg} \\ q_{sb} \\ q_{sg} \end{Bmatrix} = \begin{Bmatrix} 0 \\ 0 \\ 0 \\ 0 \end{Bmatrix}^{ext} \end{aligned} \quad (5)$$

Eq.(6) is now the summarized representation of the complete system

$$\bar{M} \ddot{\bar{q}} + (\bar{C} + \Omega \bar{G}) \dot{\bar{q}} + \bar{K} \bar{q} = F^{ext} \quad (6)$$

and this time \bar{M} represents the mass of the complete system, \bar{G} the matrix of the gyroscopic effect on rotating parts, while \bar{K} and \bar{C} consider the total stiffness and damping of the system including the contribute of the bearings.

Assuming that the external loads, coming from an unbalance analysis, are harmonic forces rotating synchronously with the rotor ($F^{ext}(t) = F_0 e^{i\omega t}$), displacements can be expressed as $u = U_0 e^{i\omega t}$, where for a multiple degree of freedom system, U_0 corresponds to the constant vector collecting modules of displacements.

The expression of Eq.(6), after the substitution of the new formulation of displacements, becomes:

$$(-\omega^2 \bar{M} + i\omega \{\bar{C} + \omega \bar{G}\} + \bar{K}) U_0 e^{i\omega t} = F_0 e^{i\omega t}. \quad (7)$$

Reduced Model

The growing of the complexity of the model to represent, drives this study to the modelling of a computationally reduced solution of the baseplate, that generally represents the most complex component considering its wide number of DOF.

At this step the baseplate is transformed in an equivalent transfer function (Vazquez 1999) and then it is necessary to choose those nodes that represent the “input/output boundary” of the equivalent formulation.

Master DOFs are as usual chosen on the boundary of the support structure and the result of this consideration tells that nodes that perfectly suit the circumstances are, as highlighted in Figure 7 and Figure 8, nodes on the bearing seat.

TEST CASE

As result of a high shaft vibration issue experienced on field on a centrifugal compressor, a great number of vibration data have been gathered on both structure and proximity probes.

The compression system (Figure 9) was made up of a gas turbine driver, two centrifugal compressors and one gearbox in one single shaft line.

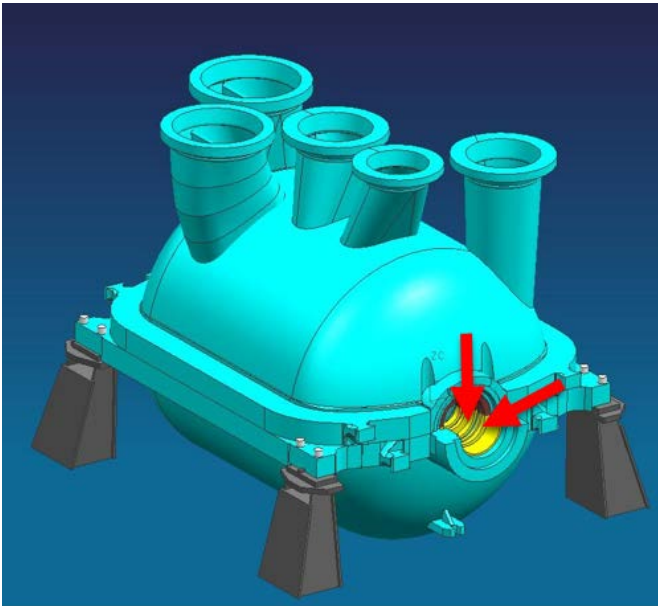


Figure 8: MCL rotor casing, bearing interface

Each rotating machine was installed on a separate baseplate steel structure and the individual rotors were connected by elastic coupling.

High vibration was detected at multi-stage, horizontally split, centrifugal compressor (MCL) at the proximity probes of both bearings, compromising the proper train start up sequence.

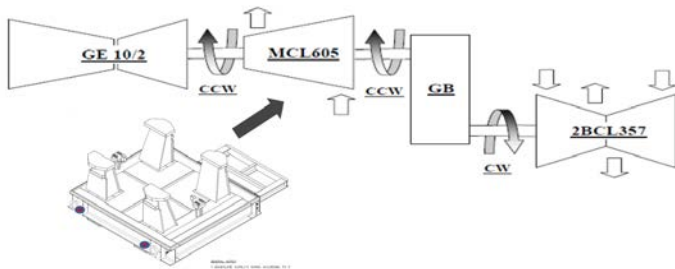


Figure 9: test case rotor train

Several accelerometer probes were positioned at the compressor pedestals, steel baseplate structure and compressor casing (Figure 10), measuring vibration level along the horizontal & vertical directions (amplitude and phase). From the preliminary vibration data acquisition on the structure, an unexpected response was revealed close to the operating speed but not to the extent to justify the train trip shut down.

The solution to the problem was implemented with the insertion of concrete underneath the baseplate to redefine a suitable anchoring system.

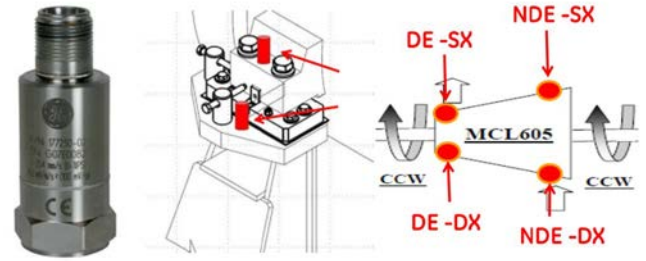


Figure 10: test rig, accelerometers arrangement

The structure mode shapes and frequencies were retrieved, using a high number of accelerometers (about 60), from a sequence of machine start up and shut down by means of a dedicated post processing procedure called Operating Modal Analysis (OMA). The extracted modes shape and frequencies were then compared to the one computed by dedicated FE models with the purpose of a better understanding of the system dynamic behavior.

Due to the complexity of the mechanical system under investigation and the strong focus on the effect of the structural dynamics on the overall shaft dynamics, a great accuracy of the baseplate FE model was fundamental for a robust experimental and numerical system validation.

Looking at the Un-damped Critical Speed map (Figure 11) the rotor exhibits a critical speed at around 3800rpm, but when evaluating the unbalance response both computationally and experimentally through the mechanical running test, this showed to be nicely damped and it could easily passed with shaft displacement lower than 20-25 μm .

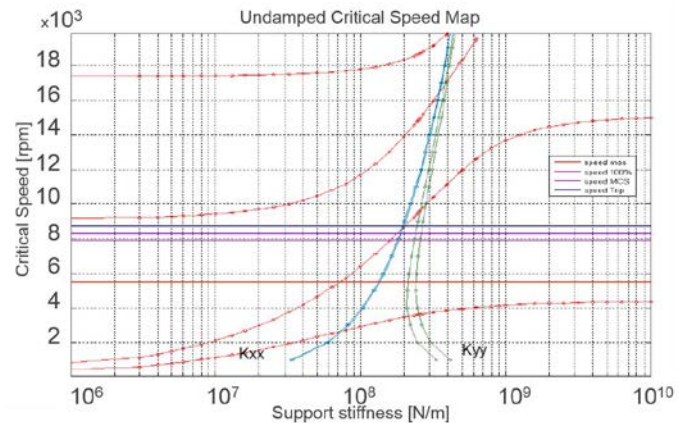


Figure 11: Undamped Critical Speed Map

In Figure 12 it is shown how the response of the baseplate changes as consequence of the degree of constrain at the anchorage to the ground, and how the resonance peak shifts in frequency following the increasing stiffness of the different solutions.

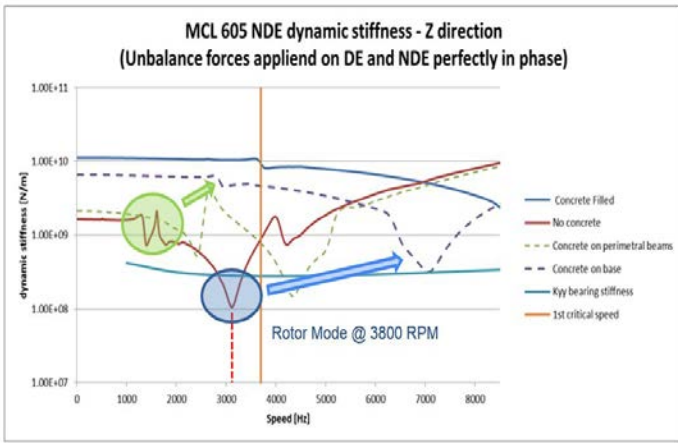


Figure 12: possible solutions, comparison on support structure dynamic stiffness

The dynamic stiffness (N/m) of the implemented solution and the original one are compared in Figure 12, where stiffness is reported as a function of the shaft rotating speed, as result of synchronous forces placed at the bearing interface: Anchorage by only 4 foundation bolts (original configuration); Grouting to the baseplate perimeter (easy to implement); Grouting the entire lower surface of the structure.

In Figure 12 there is the evidence of a structural mode in the operating range where the vertical stiffness (K_{yy}) degrades below the bearing stiffness around 3000 rpm. In particular, it is possible to note how the separation margin between the rotor critical speed and the characteristic of baseplate, can be increased by implementing a proper anchoring solution.

MAJOR FINDINGS

Following the guide lines reported above it is interesting to see the difference in the rotor response (Figure 13) before (No Grouting) and after the concrete reinforcement (Grouting). The response of the rotor with bearing constrained to an infinitely rigid support (Figure 13, rotor) is compared with the real configuration where the dynamic of the rotor is coupled with the dynamic of the support structure.

Comparing Figure 12 and Figure 13 one can see the effect of the structural dynamic response change after the implementation of the grouting solution. This introduces a frequency shift of the critical speed (few hundred of RPM) and a smoother response curve as seen from the rotor lateral analysis. Furthermore, it is possible to recognize the resonance peak of the baseplate around 3000rpm (Figure 13, No Grouting curve) where the amplitude of displacements grows exponentially. What is worthwhile to highlight is the relevance of the non-optimal anchorage of the baseplate that allows an unwanted elastic capability of the support structure, enhancing the importance of cross-talking terms in the stiffness transfer matrix.

The Bentley Nevada proximity probe reading gathered during the test done in the grouting configuration (Figure 15), is extremely well matching the outcome of the simulated system (Figure 13, Grouting curve) as confirmation of the accuracy of the performed analysis.

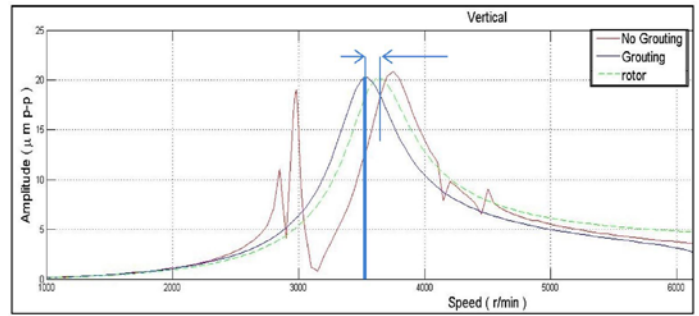


Figure 13: vertical relative displacements, effect of concrete reinforcement

Comparing the response of the rotor mounted on the simplified baseplate model, that is to say a baseplate representation ignoring cross-talking terms (Figure 14), the behavior of the real system (rotor plus structure) converges to the case where the support is assumed infinitely rigid. This is the true evidence that ignoring the cross talk element of the dynamic stiffness matrix can lead to erroneous results.

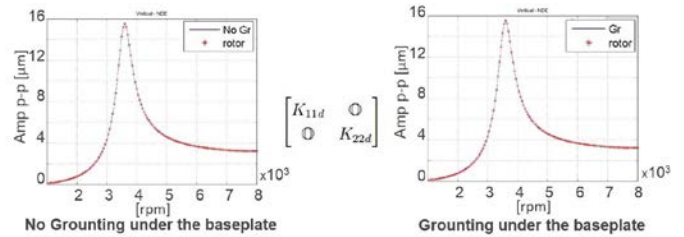


Figure 14: influence of cross-talk terms

When comparing the results of the computational study (Figure 12) with the system response retrieved from the experimental modal analysis (Figure 16), one can see some correspondences and some apparent mismatch.

This due to the discretionarily assumption on the loading characteristics used to obtain the stiffness plot, which might potentially not help in highlighting all possible resonances.

Looking the waterfall plot (Figure 16), a presence of the support structure resonance around 4080 RPM after the concrete reinforcement is clearly visible, however the signal amplitude is not increasing while crossing with the 1 x Rev excitation indicating the mode as not affecting the bearing stiffness's characteristics. This mode is not affecting the rotor dynamic solution (Figure 15).

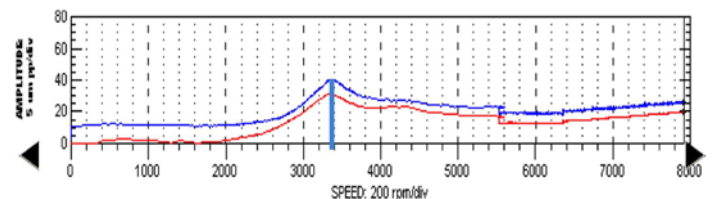


Figure 15: Bentley Nevada, relative displacements

The operational modal analysis (OMA) was then conducted to experimentally reconstruct the deformed shapes of the system modes through a number of accelerometers placed on both compressor casing and supporting structure. This technique helped us to understand the compressor motion as excited by

the unbalance loading and compare it with the acquisition from proximity probes and computational prediction.

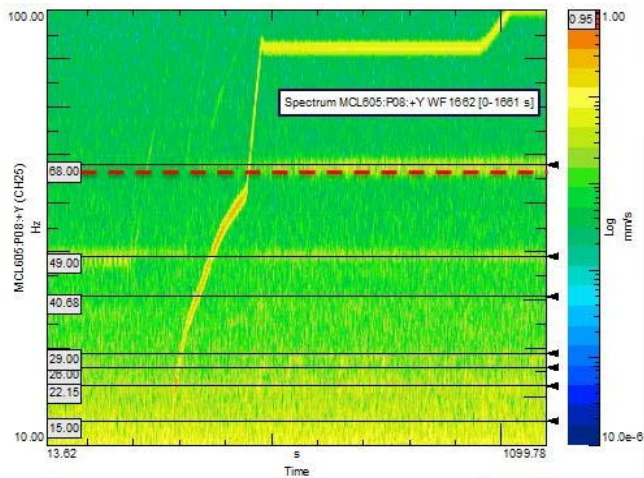


Figure 16: waterfall diagram

In Figure 17, the deformed shape of the resonance mode at around 1800 rpm is showing displacement predominantly in the axial direction with slight contribution laterally. This will not have any major effect on the rotor dynamics due to the low modal participation along the vertical and lateral directions.

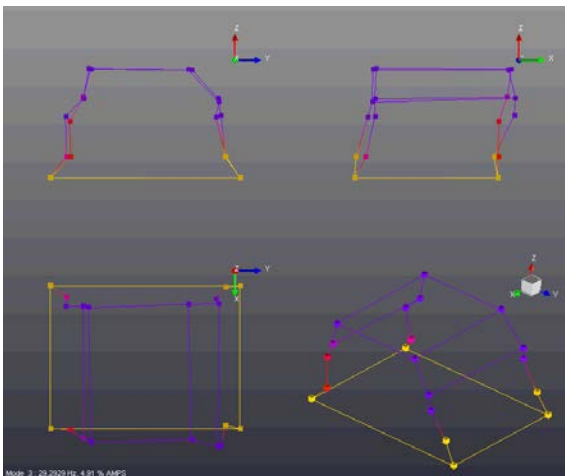


Figure 17: OMA, 29Hz – 1740rpm

Similarly, in Figure 18, the deflected shape at 68 Hz (4080RPM) cannot be easily excited with a centered rotor unbalance as it shows a rotation of the compressor casing along the shaft axis and some additional contributions along the vertical and lateral direction. Modal shapes must always be seen in connection with their participation to the system excitation.

CONCLUSIONS

Including the support structure dynamic in the rotor-bearing system, just through the use of the diagonal terms of the stiffness matrix (“direct stiffness”) can lead to a wrong rotor dynamic assessment. Weak anchoring solution can enhance the importance of cross talk terms, which can drive the system to modify the rotor response.

While approaching new trends in the O&G industries, as weight reduction for off-shore compression trains, special care must be taken in the structural\rotor dynamic integration.

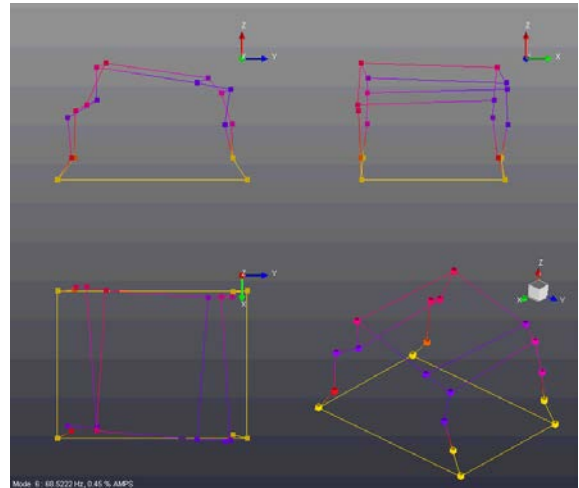


Figure 18: OMA, 68Hz – 4080rpm

GE Oil&Gas is moving to the definition of complex transfer functions to efficiently couple the rotor dynamic with structure dynamic. Currently under investigation the effects of machines foundation as coupling element between rotating elements (GT-GB-CC) in the same shaft line.

The importance of a combined analysis of rotors and elastic supporting structure arises with the continuous development of turbo machinery applications, in particular in the Oil & Gas field where a wide variety of solutions, such as off-shore installations or modularized turbo compression and turbo generator trains, lead to the need of a more complete study with strong focus on the whole system assembly not only limited to the rotor/bearing system.

Complex elastic systems in some situations might strongly dominate the entire shaft line rotor dynamic response (mode shapes, resonance frequencies and unbalance response). They give the birth to transfer functions which introduce strong coupling phenomena between machines bearings, becoming enablers of a new shaft line dynamics.

Unlike established procedures based on existing methodologies often requiring expensive computational time and/or unwanted level of detail, this work attempts to rise the requirement of a new method leveraging a high level of accuracy / high computationally efficient method emphasizing a valuable match between experimental and numerical results which confirms the importance of a proper definition of the complex transfer function.

With this work GE Oil & Gas is revealing the strong capability of system integration for rotating machines, consistently improving the structural design over the year extending the connection to the shaft line rotor dynamics. New tools have been developed to make this possible for every project whenever required.

Ge Oil&Gas is currently performing a number of test campaigns to validate the procedure. As we move forward increasing the rotor speed and the compressor power, the integrated structural-rotor dynamics becomes a must.

REFERENCES

- K. Cuppens, P. Sas and L. Hermans, Evaluation of the FRF Based Substructuring and Modal Synthesis Technique Applied to Vehicle FE Data, Department of Mechanical Engineering, Division PMA, ISMA International Conference on Noise and Vibration Engineering, September 2000, pp.1143-1150.
- D. Brugier, M.T. Pasal, Influence of elastic deformations of turbogenerator tilting pad bearings on the static behavior and on the dynamic coefficients in different designs, ASME J. Tribol., Vol. 111, No. 2 , pp. 364-371, ISSN: 0742-4787, 1989.
- J. Vazquez and L. Barrett, Transfer Function Representation of Flexible Supports and Casings of Rotating Machinery, Department of Mechanical Engineering, Division PMA, sem.org IMAC XVII 17th, 1999.
- T. Kruger, S. Liberatore e E. Knopf, Complex Substructures and Their Impact On Rotor Dynamic, SIRM 2013 - 10th International Conference on vibrations in Rotating Machines, 2013.
- K.L Cavalca, P.F Cavalcante, E.P Okabe, An investigation on the influence of the supporting structure on the dynamics of the rotor system, Mechanical Systems and Signal Processing, Volume 19, Issue 1, January 2005, Pages 157-174, ISSN 0888-3270.
- Y. Kang, Y.-P. Chang, J.-W. Tsai, L.-H. Mu, Y.-F. Chang, An investigation in stiffness effects on dynamics of rotor-bearing-foundation systems, Journal of Sound and Vibration, Volume 231, Issue 2, 23 March 2000, Pages 343-374, ISSN 0022-460X.